A NUMERICAL SIMULATION OF THE 1991 LIMÓN, COSTA RICA, EARTHQUAKE[1]

Aarón Moya[2]

ABSTRACT: Synthetic strong motion records for the 1991, Mw 7.6, Limón, Cosa Rica earthquake were computed for several hundred different source models. The rotd50 (response spectra) was used to compare synthetic and observed data at seven stations that recorded the event. The source model that minimized the misfit was selected to calculate new synthetic records at present-day stations. The result indicated that the fault length reached some 100 km long by 40 km deep. The largest peak ground acceleration would have been recorded in the stations located along the Caribbean coast, close to the epicenter. A post-earthquake bridge inspection calculation using our scenario earthquake predicted a high level of damage to several bridges that collapsed in 1991.

Keywords: bridge collapse, Limón 1991 earthquake, seismic intensity, strong motion, synthetic simulation

SIMULACIÓN NUMÉRICA DEL TERREMOTO DE LIMÓN DE 1991, COSTA RICA

RESUMEN: Se calcularon registros sintéticos de movimiento fuerte para el terremoto de 1991, Mw 7.6, Limón, Costa Rica usando varios cientos de modelos de fuentes diferentes. El rotd50 (espectro de respuesta) se utilizó para comparar datos sintéticos y observados en siete estaciones que registraron el evento. Se seleccionó el modelo fuente para el cual la diferencia entre los registros sintéticos y observados fuera mínima. Con este se calcularon nuevos registros para estaciones en la actualidad. El resultado indica que la longitud de la falla alcanzó unos 100 km de largo por 40 km de profundidad. La aceleración máxima se habría registrado en las estaciones ubicadas a lo largo de la costa caribeña y cerca del epicentro. Un modelo de cálculo de inspección de puentes post-terremoto utilizando el escenario seleccionado, predijo bastante bien el alto nivel de daño y colapso de estructuras observado en 1991.

Palabras claves: colapso de puentes, movimiento fuerte, intensidad sísmica, simulación sintética, terremoto de Limón de 1991

INTRODUCTION

On April 22nd, 1991, a magnitude Mw 7.6 earthquake struck the Caribbean coast of Costa Rica. The event was unexpected as the subduction zone, which is the source of most earthquakes in the country, was located on the Pacific coast. This earthquake was caused by reverse faulting along the North Panama Deformed Belt (NPDB) (Plafker and Ward, 1992; Suárez *et al.,* 1995). The epicenter was located on the Valle La Estrella, a scarcely populated mountain region of difficult access in the province of Limón. The rupture extended from Limón city in Costa Rica to the Bocas del Toro province in Panama.

There was extensive damage to man-made structures, especially in *Limón* province; several dozen people died in both countries. Communications were disrupted because of lateral spreading of soils, liquefaction, and landslides that destroyed roads and collapsed bridges (Morales, 1994; Santana, 1994). Water and oil pipelines were damaged (O'Rourke and Ballantyne, 1992; EERI, 1991; Santana, 1994). A small tsunami was observed with runup up to 1m in Cahuita, in Costa Rica and 3 m on the Panama side (Chacón-Barrantes

[1] Article received on October 11, 2021 and accepted for publication on November 1, 2021.
[2] Associate Researcher, Seismic Engineering Laboratory, University of Costa Rica. San Pedro Montes de Oca, San José, 11501, Costa Rica. Email: aaronmoya@gmail.com

and Zamora, 2017). The earthquake also uplifted the coast over 1 m in certain regions (Denyer *et al.,* 1994) exposing the coral reefs and changing the relief.

Suárez *et al.,* (1995) identified other major events with magnitude larger than 7.0 along the NPDB: 1822, 1916, and 1991. They even suggested that the moment release in the Caribbean coast could be comparable to that of the subduction zone along the Pacific. According to Boschini and Montero (1994) the earthquake of 1822 shared similar macroseismic characteristics as the 1991 event. Considering this, it seems that large earthquakes are common in the area, but could have long return periods which make them difficult to study.

We computed synthetic seismograms for different source models for the 1991 earthquake. We varied the focal mechanism and fault dimensions in order to find the best model that could explain the few observed records from 1991. We then created an intensity map and examined the impact that a similar earthquake could have on several of the bridges on national highway 32 and 36.

STRONG MOTION STATIONS

The Earthquake Engineering Laboratory at the University of Costa Rica (LISUCR) operates a strong motion network of over 100 stations. They are all digital 24 bit accelerometers that are used to calculate earthquake source and engineering parameters. The current day station location covers most of the country. However, in 1991 there were only 19 permanent stations equipped with Kinemetrics SMA-1 analog accelerometers. Some stations were inside high-rise buildings and others in free-field condition.

The stations were located along the subduction zone in the Pacific coast and the Central Valley following the 1986 edition of the Costa Rica Seismic Code (CSCR-86). At that time, it was believed that the Caribbean coast had a low seismic potential (Quesada-Román, 2016; Suárez *et al.,* 1995) because of the low seismicity rate since the instrumental recording began. The closest station to the epicenter was SISD (Figure 1) located 78 km away.

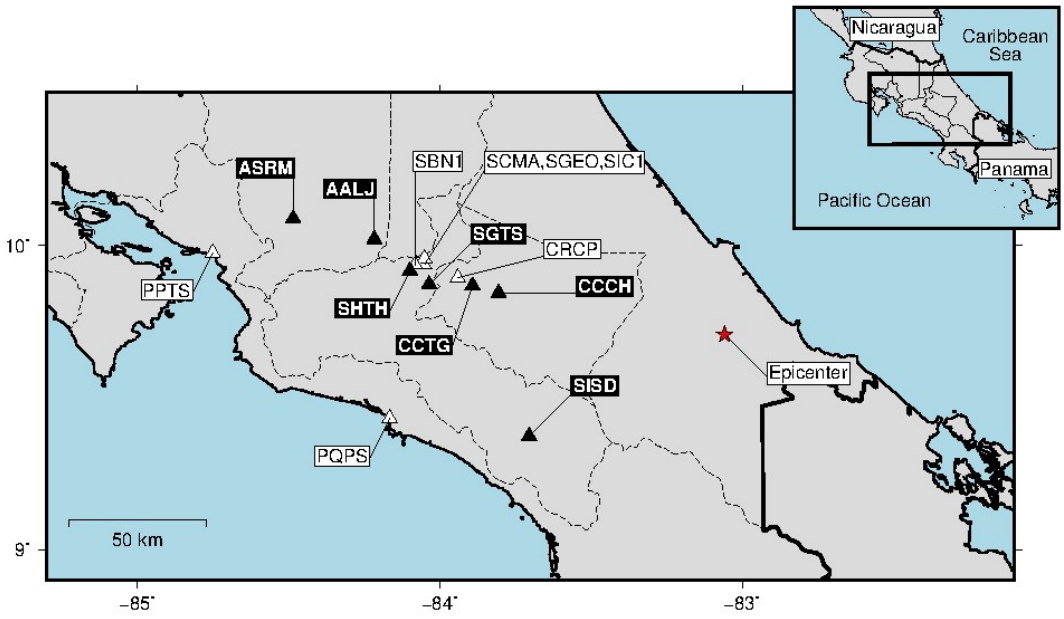

Figure 1: Strong motion station distribution in 1991. Black triangles correspond to the free-field stations used in this study. The red star shows the epicenter of the earthquake.

Analog instruments were triggered by a given amplitude threshold. The threshold was reached after the waveforms had already arrived at the station. That caused the pre-event and part of the P-wave information to be missing. On occasions, the record would also be incomplete because of power outage or high humidity in the station that would hinder the recording film. In addition to that, the records had to be filtered in the range 0.8 – 23 Hz due to the instrument's mechanical limitations and post-processing of signals. Based on those characteristics, out of the fourteen stations that recorded the Limón earthquake (Santana, 1994), we selected only seven of them.

Figure 1 shows the station distribution in 1991. Table 1 shows the name given to the sites and their current location. Five of stations are still in the same place as in 1991. CCTG and AALJ were located near the central park of Cartago and Alajuela cities respectively. Both stations had to be moved to different places due to remodeling of the parks. SISD was the closest station to the epicenter, 78 km away, and recoded a peak ground acceleration (PGA) = 190 gals. CCTG was located 92 km away from the epicenter and recorded a PGA=256 gals.

SYNTHETIC SEISMOGRAMS

We carried out several hundred simulations using the SCEC Broadband Platform (BBP) version 19.4 (Maechiling *et al.,* 2015) for the stations listed in Table 1. The SCEC BBP is an open-source set of programs that combines the effects of source, path, and site effects to produce a realistic record of the ground motion. The software contains seven simulation methods that can generate synthetic records from 0 to 20+Hz. In this study, we used the GP method (Graves and Pitarka, 2015) in which the ground motion model is implemented in three processing stages: a rupture generator stage, a low frequency deterministic stage, and a stochastic high frequency stage (Baker *et al.,* 2014).

Table 1: List of selected stations that recorded the 1991 earthquake and present day location.

Code	Station location in 1991	Code	Stations used in this study
AALJ	Alajuela Central Park	AALA	Moved to the office branch of INS
ASRM	San Ramon, UCR	ASRM	San Ramon, UCR. (Same location)
CCCH	Cachi dam	CCHI	Cachi dam. (Same location)
CCTG	Cartago Central Park	CCRT	Moved to Cartago Public Library
SGTS	Guatuso primary school	SGTS	Guatuso primary school. (Same location)
SHTO	Hatillo Clinic	SHTH	Hatillo Clinic. (Same location)
SISD	Office branch of INS	SISD	Office branch of INS. (Same location)

The BBP has several built-in region-specific velocity models for North America and Japan (Maechiling *et al.,* 2015). In order to compute synthetic seismograms for other parts of the world, it is necessary to assume a similar model to the ones provided by the distribution. In this case, we selected the Central Japan velocity model since it is probably the one that most resembles the tectonic environment in Costa Rica. Superficial site effects were given by the *Vs30* parameter. The LISUCR computed *Vs30* for several stations by conducting direct field measurements (Schmidt, 2014). In other cases, the *Vs30* was derived from the topographic slope (Heath *et al.,* 2020). It is assumed that a gentle slope correlates with alluvial plains and sedimentary basins, where there is a low shear wave velocity.

The source model in BBP is described by the earthquake's magnitude, depth, focal mechanism, and fault dimensions. A different source model was used for each simulation. According to Leonard (2010), a M_w 7.6 event would rupture a 102 x 38 *km* rectangular fault. Montero *et al*. (1994) indicated that the rupture area from the aftershock distribution could reach 85.45 km^2. We iterated through a 100, 120, and 130 *km* fault length and 40 and 45 *km* fault width.

Depth to the upper part of the fault was computed for 5 and 10 *km*. The focal mechanism was taken from Goess *et al*. (1993) (strike 103, dip 25, and rake 58). It was changed by 5 degrees along the strike, dip and rake angles. A total of 750 simulations were conducted by iterating through the different parameters. We used a random seed for every new source model each time.

Three component synthetic seismograms were computed. They were filtered in the range 0.8 – 23 *Hz* in order to match the observed records. Then we calculated the rotd50 spectrum for each site and compared the synthetic result to the observed one.

We estimated the error using the following formula

$$error = \sum_{i=1}^{n} \frac{(syn_i - obs_i)^2}{\sqrt{(syn_i * obs_i)}} \quad (1)$$

where *i* is the *period*, *syn* is the synthetic spectrum and *obs* the observed one.

RESULTS

Simulation number 607 yielded the smallest error. The plots of the rotd50 for the observed and synthetic records are shown in Figure 2. The resulting fault from model 607 is 100 *km* long by 40 *km* deep. Plafker and Ward (1992) estimated the rupture to be 40 *km* wide by 80 *km* long. The strike, dip, and rake of the focal mechanism are 103, 30, and 58 respectively. The depth to top of the fault is 10 *km* which means that the hypocenter is located at 16.8 *km* deep. Figure 2 shows the fault projection on the map. The maximum slip is 6 *m*.

Figure 3 shows the *rotd50* (5% damping ratio) for the synthetic records from the selected source model. In general, the simulation results yielded lower spectra values than the observed records. Only station CCCH and SGTS showed similarities in amplitude. CCCH is located inside a tunnel close to the Cachi dam. The tunnel is drilled inside basalt, so this is a rock site. On the contrary, SGTS is a soft-soil site. The biggest differences were observed at AALJ and ASRM which were also the farther away stations. In addition to that, the stations were located on the western side of the Central Valley, In general, stations located on the western side of the Central Valley experienced important amplification during the M_w 7.6, 2012 Nicoya earthquake according to Schmidt *et al.,* (2014).

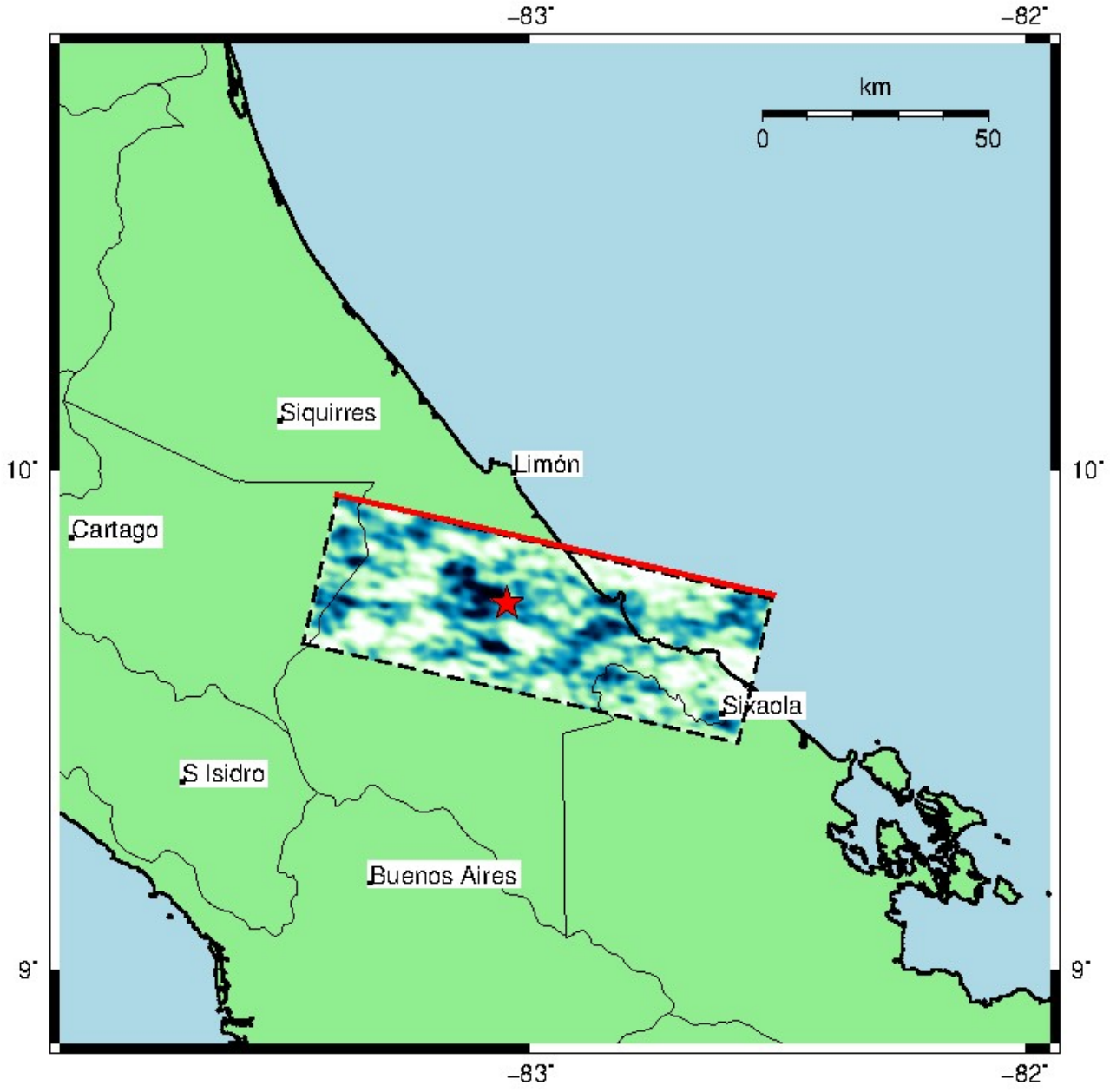

Figure 2: Fault model projection on the map. The length is 100 km and the width is 40 km. Dark areas correspond to zones of maximum slip (up to 6 m). The red line is the fault trace and the dotted line the projection at depth.

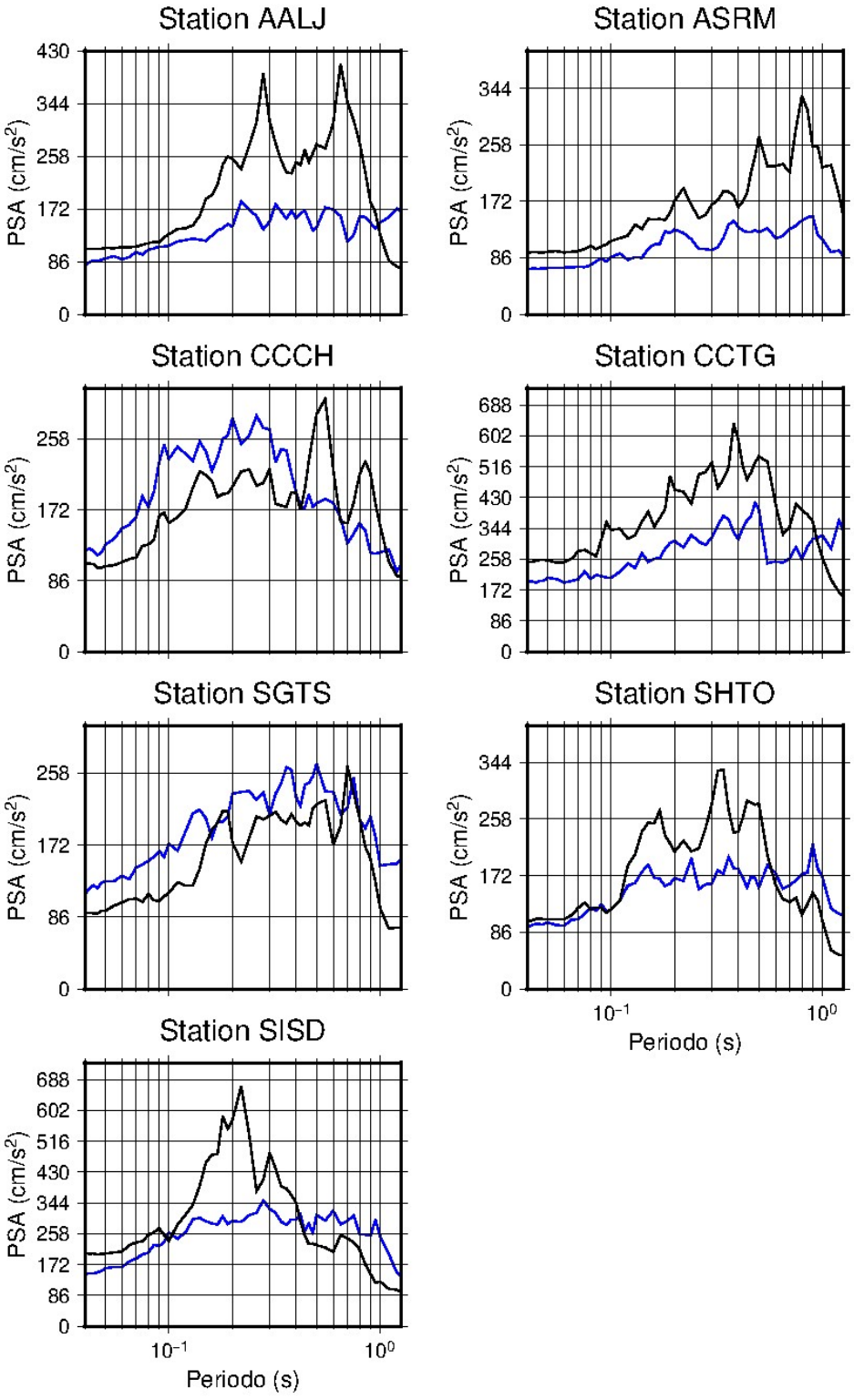

Figure 3: Synthetic (blue) and observed (black) rotd50 parameter for stations listed in Table 1.

Intensity

Overall amplitude and duration in time domain share more similarities between synthetic and observed data. Figure 4 shows the synthetic (blue) and observed (black) waveforms for the east-west (EW) and north-south (NS) components.

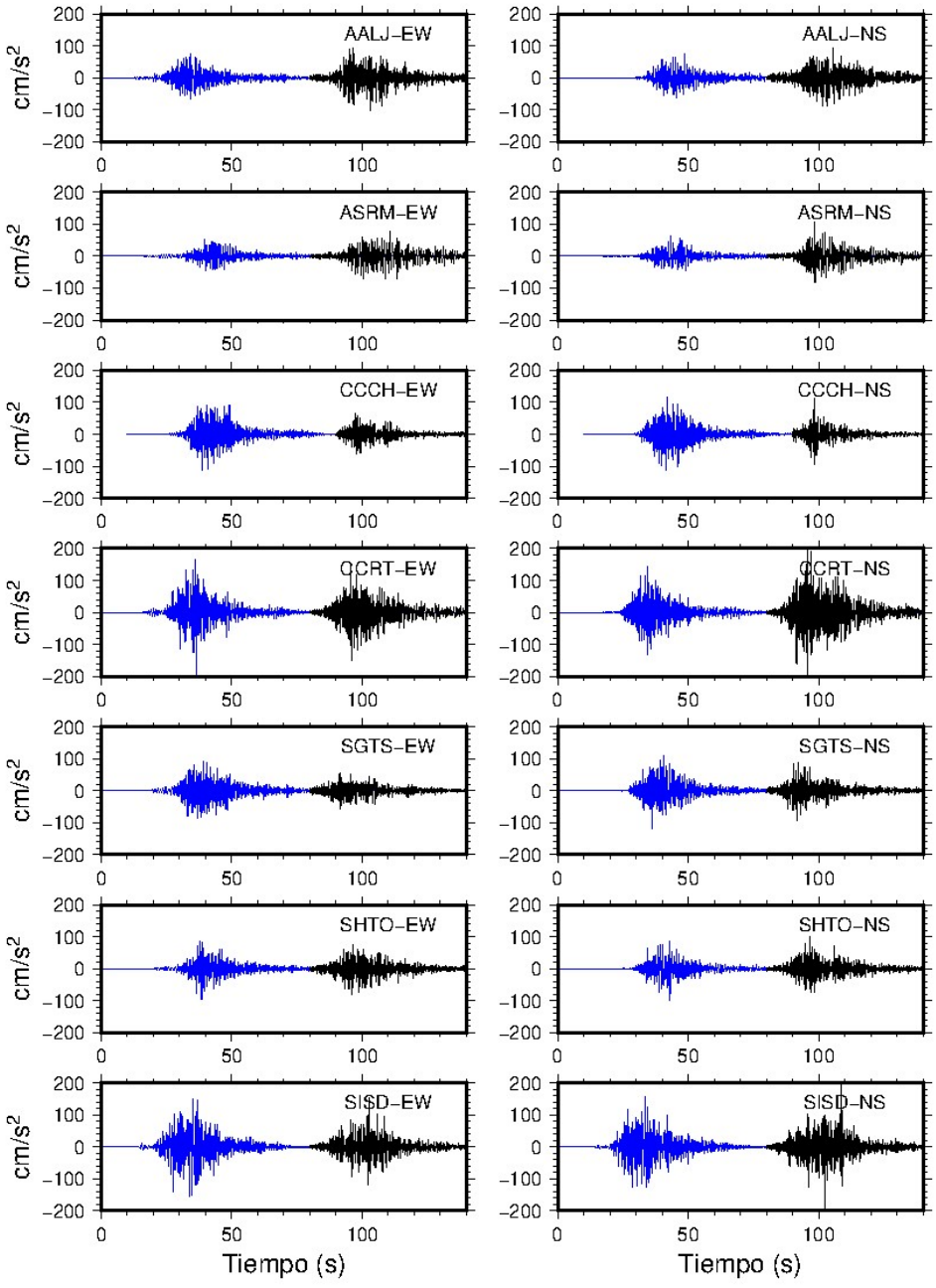

Figure 4: Waveform for synthetic (blue) and observed (black) EW and NS components.

In Table 2 the PGA and Japan Meteorological Agency's intensity scale (JMA) (Shabestari and Yamazaki, 2001) for the target stations are shown. In JMA, the three-component strong motion records are filtered in the frequency domain. Then, the vectorial summation is calculated in time domain. The value *a0* from the cumulative amplitude above 0.3 *s* is taken into the following equation

$$I_{JMA} = 2.0 \log (a0) + 0.94 \quad (2)$$

The reason we used the JMA intensity as parameter for comparison was that we could use the whole waveform from the three components for its estimation. This allowed us to compute the JMA intensity even for the 1991 stations (see Table 2).

Table 2: Observed and synthetic PGA and JMA values for selected stations

	Observed		Synthetic	
Station	**PGA (gals)**	**I_{JMA}**	**PGA(gals)**	**I_{JMA}**
AALJ	108	5-	97	5-
ASRM	92	5-	75	5-
CCCH	138	4	148	5-
CCTG	256	5+	163	5+
SGTS	102	4	131	5-
SHTO	118	5-	91	5-
SISD	190	5-	183	5+

In the JMA scale, only the observed records from CCCH, SGTS, and SISD are one degree lower with respect to the synthetic ones. In the rest of the stations from Table 1, the correspondence is one to one. The largest PGA difference happened in CCTG. The observed PGA was almost 1.5 times higher than the synthetic one. In 1991, this was the largest PGA recorded from observed records even when the station was not the closest one.

Using the same source model, we computed synthetic seismograms for another 90 sites. They correspond to present-day strong motion stations. Figure 5 shows their location along with their corresponding JMA intensity value.

For practical reasons, we re-classified or grouped levels of intensity 0, 1, and 2 into "Weak" category. They are usually related to very small shaking ranging from the instrumental level up to the perception from people at rest. Levels 3 and 4 were given the "Moderate" category. They are the levels when people start feeling the earthquake and when hanging objects move. Levels 5- and 5+ were given the "Strong" category. This is when things start to fall down. Finally, the upper levels 6-, 6+, and 7 were classified as "Very strong" shaking, this is when serious damage can occur such as liquefaction, landslides and collapse of structures.

According to this result, the Caribbean coast experienced strong shaking at Limón city with a value of JMA=5+. There was very strong shaking with JMA intensity values 6-, 6-, and 6+ in Batan, LVES (Valle La Estrella) and LTAL (Talamanca) respectively. This means that intensity in the Modified Mercalli Scale reached values between VIII and X. The largest acceleration, PGA=538 *gals* (0.548g), was recorded in Talamanca station.

The Nicoya earthquake, M_w 7.6, was another large event that struck the country on the Pacific coast in 2012 (Protti *et al.,* 2014). It was recorded by all the LISUCR digital stations at that time (Schmidt *et al.,* 2014). From the observed records, Moya (2018) estimated that the largest JMA value was 6-. One particular site, ASRM,

reported a JMA= 6- at 120 *km* away from the epicenter. The JMA= 6- and 6+ obtained for LVES and LTAL seem to be reasonable values considering that the stations are located on top of the rupture area.

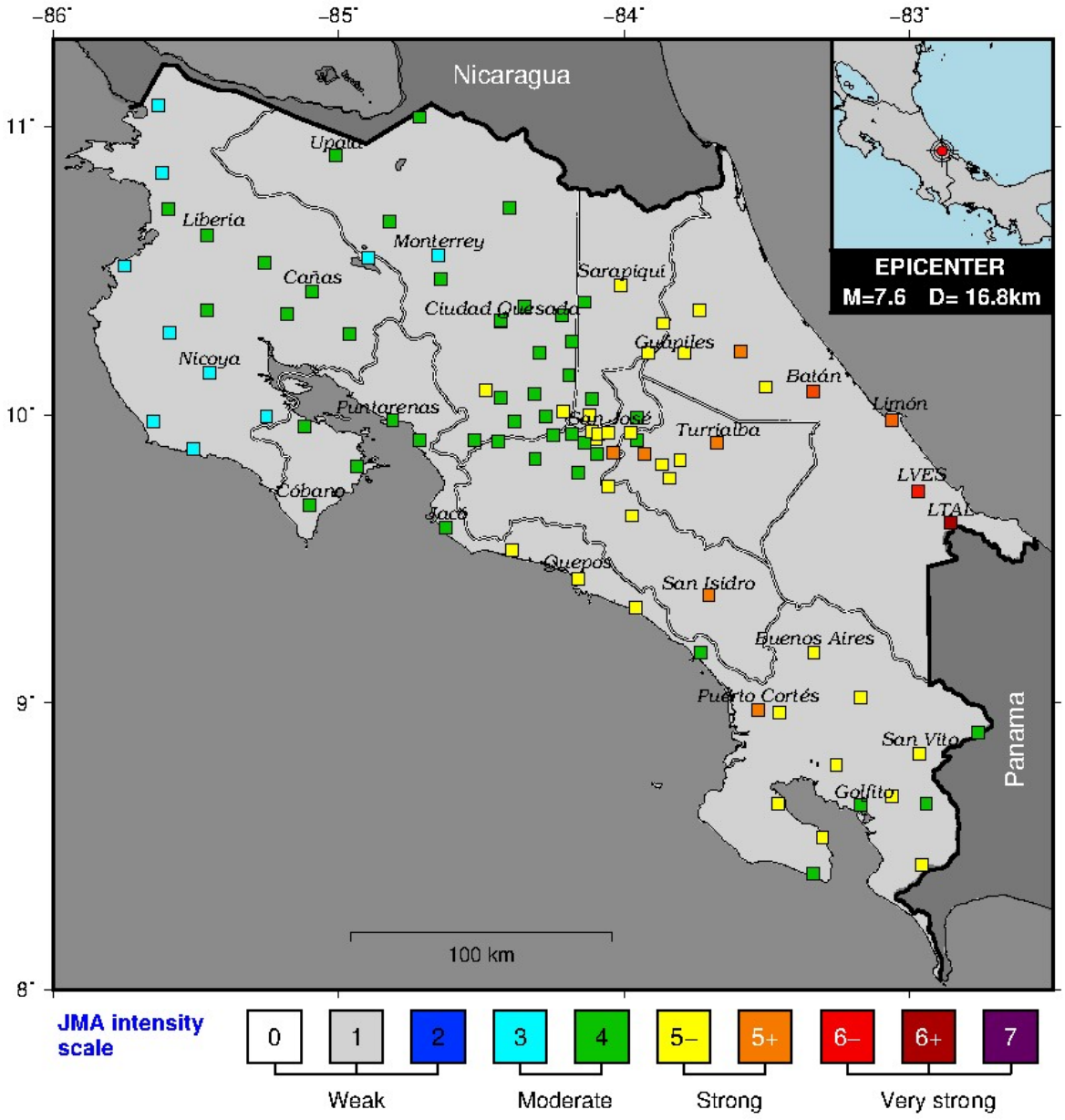

Figure 5: JMA intensity for 97 strong motion stations calculated from the selected source model.

The most important city on the Caribbean coast is Limón. The hospital and several hotels in the region suffered severe damage, even partial collapse (Santana, 1994). Figure 6 shows a comparison between the synthetic (red and blue lines) and the design spectra from the CSCR-2010 in the city (green line). Spectral values from the actual scenario earthquake clearly surpassed the design spectral level at around 0.8 *s*.

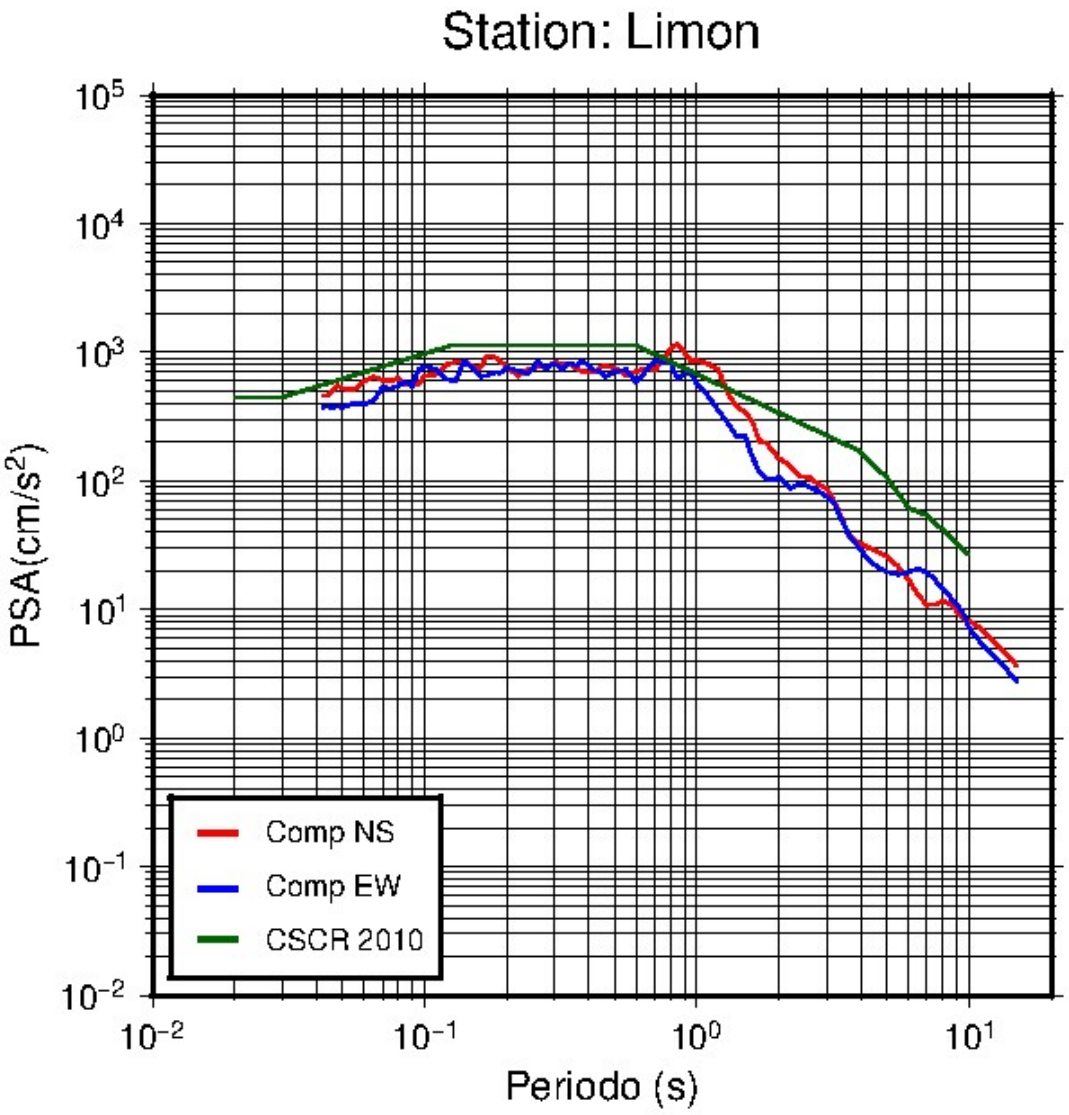

Figure 6: Design spectra (green) and synthetic NS (red) and EW (blue) for at the city of *Limón*.

Bridges

Highways 32 and 36 are the most important access to the Caribbean coast. Five bridges completely collapsed and several others were severely damaged during the earthquake. On highway 32, the west-end span of the bridge on the Chirripo river, the longest bridge at that time (Morales, 1994) collapsed due to loss of support (Sauter, 1994; Santana, 1994). This alone made nearly impossible to reach Limón city by land for four days (Morales, 1994). Bridges on the Rojo, Toro, Cuba, and Blanco rivers were also highly damaged. On highway 36, from Limón city to Talamanca, the bridge on the Vizcaya, Bananito, and Estero Negro rivers also collapsed. Sauter (1994) indicates that most of the collapsed structures were located on soft alluvial and saturated soils.

Muñoz-Barrantes *et al*. (2017) developed a methodology for post-earthquake bridge safety inspection. They created a database of 1400 bridges containing information related to the structural characteristics as well as their vulnerabilities. After a strong earthquake, they calculated the expected damage to the structures by using fragility curves. The calculation took into account the different soil conditions and liquefaction potential where the bridges were located. The main purpose of this tool is to provide preliminary information on where the emergency response efforts should be aimed when there is a strong earthquake.

The methodology was coded into the LISUCR's automatic monitoring system (SMA-LIS). The SMA-LIS goes off when a strong earthquake is detected by the network. After calculating several strong motion parameters, such as the response spectra, the SMA-LIS creates a map with the different attention levels that should be given to every bridge in the database. There are five inspection levels: "Non priority inspection", "Exploratory inspection", "Priority exploratory inspection", "Priority safety inspection", and "Urgent safety inspection."

Figure 7 shows the result for the Muñoz-Barrantes *et al*. (2017) methodology after using our earthquake scenario as input. In general, all bridges along highway 32 turned out in orange, meaning they would require a "Priority safety inspection" after the earthquake. Two of the most important ones, Chirripo and Vizcaya, turned out in red. They would require an "Urgent safety inspection."

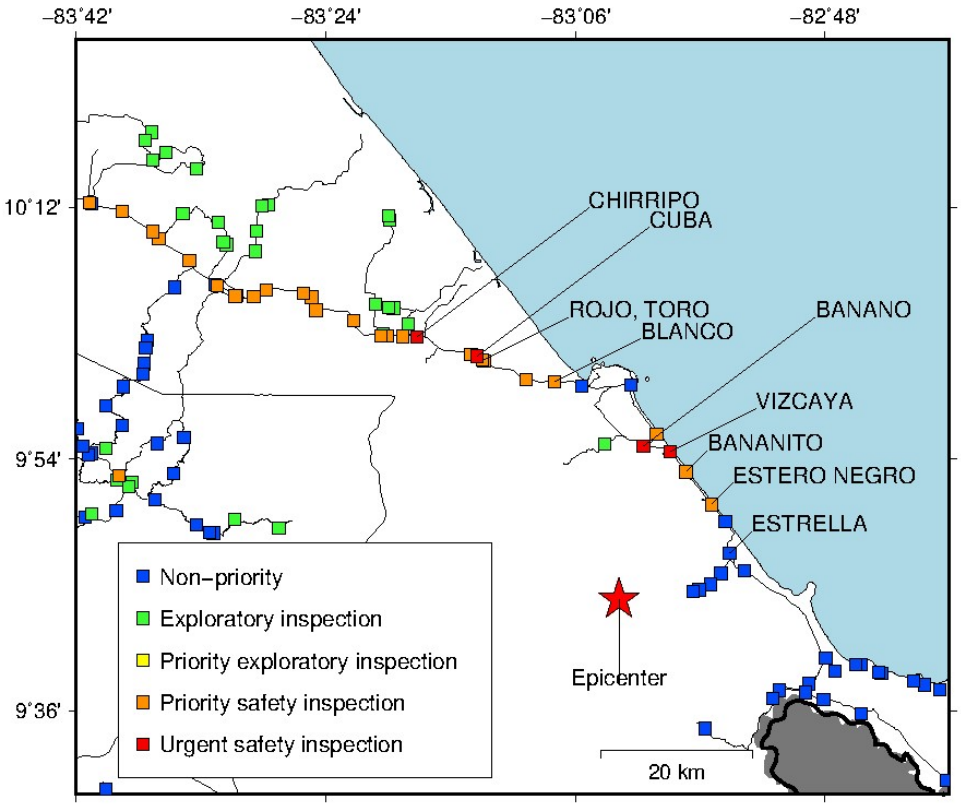

Figure 7: Calculation result for the post-earthquake bridge inspection from Muñoz-Barrantes (2017) methodology.

The bridge on the Banano river did not collapse, but it turned out in red in our result. However, its foundation was severely damaged according to Sauter (1994). On the other hand, the bridge on the Estrella river turned out in blue in this study, but it was one of the damaged structures.

CONCLUSIONS

To this day, the *Limón* earthquake remains of the most destructive earthquakes in Costa Rica for which there was very few strong motion records. We have calculated an intensity map based on synthetic data from a realistic earthquake source model using the BBP. The observed and synthetic data were compared using the rotd50 spectra. The waveforms were also compared for the PGA. The best model was used to obtain strong motion records at present-day station locations.

The result seems to be good at closer epicentral distances. At some sites, especially those farther away from the epicenter, stronger site effects probably need to be considered. On the other hand, the results can be improved by using a velocity model for the country. In this study, we used the one for Central Japan assuming the tectonic environments were similar. The amplitude mismatch observed at some stations, could also be related to differences in attenuation.

Difference for the JMA estimation at some sites could be due to the record's length. JMA takes into account not only the amplitude but also the duration of the signal. Since the observed records are shorter than synthetic ones (because of the threshold value used and the signal's cut off), there is less information for the calculation of JMA.

The largest values of JMA intensity happened along the Caribbean coast and affected specially roads and bridges on highway 32 and 36. Our result seems to explain the damage to the most important bridges that collapsed in 1991. This could be used to predict strong ground motion for a potential future earthquake in the same region.

ACKNOWLEDGEMENTS

This work has been possible thanks to the funding from the National Emergency Law to the Earthquake Engineering Laboratory. Maps and graphics were made with the GMT software (Wessel *et al*, 2013), and much of the processing was done with the SAC software (Goldstein *et al*, 2003).

REFERENCES

Baker, J. W., Luco, N., Abrahamson, N. A., Graves, R. W., Maechling, P. J., and Olsen, K. B. (2014). "Engineering uses of physics-based ground motion simulations." Proceedings of the 10th National Conference in Earthquake Engineering, Earthquake Engineering Research Institute, Anchorage, AK.

Boschini, I.M., and Montero, W. (1994). "Sismicidad histórica e instrumental del Caribe de Costa Rica." Revista Geológica de América Central, Volumen Especial del Terremoto de Limón. (pp. 65-72).

Chacón-Barrantes, S. and Zamora, N. (2017). "Numerical Simulations of the 1991 Limón Tsunami, Costa Rica Caribbean Coast." Pure and Applied Geophysics, 174(8), 2945–2959. Doi: 10.1007/s00024-017-1631-x.

Denyer, P., Arias, O., and Personius, S. (1994). "Efecto tectónico del terremoto de Limón". Revista Geológica de América Central, Volumen Especial del Terremoto de Limón. (pp. 39-52).

Earthquake Engineering Research Institute (EERI) (1991). “Costa Rica earthquake of April 22, 1991 Reconnaissance Report”, Earthquake Spectra, 7, supp. B, 127pp.

Goes, S., Velasco, A., Schwartz, S., and Thorne, L. (1993). “The April 22, 1991, Valle La Estrella, Costa Rica (M_w=7.7) earthquake and its tectonic implications: A broadband seismic study.” Journal of Geophysical Research, Vol 98. No. B5, pp 8127-8142.

Goldstein, P., Dodge, D., Firpoand, M., and Lee Minner, S. (2003). “SAC2000: Signal Processing and Analysis Tools for Seismologists and Engineers”, Invited contribution to “The IASPEI International Handbook of Earthquake and Engineering Seismology”, Edited by WHK Lee, H. Kanamori, P. C. Jennings y C. Kisslinger, Academic Press, London.

Graves, R. and Pitarka, A. (2015). “Refinements to the Graves and Pitarka (2010) broadband ground-motion simulation method”. Seismological Research Letters, 86: 75–80.

Heath, D., Wald, D. J., Worden, C. B., Thompson, E. M., and Scmocyk, G. (2020). “A Global Hybrid Vs30 Map with a Topographic-Slope-Based Default and Regional Map Insets”, Earthquake Spectra, Vol. 36, 3: pp. 1570-1584.

Leonard, M. (2010). “Earthquake fault scaling—Self-consistent relating of rupture length, width, average displacement, and moment release”, Bulletin of the Seismological Society of America, Vol. 100, No. 5A, p. 1971–1988.

Maechling, P. J., Silva, F., Callaghan, S., and Jordan, T. H. (2015). “SCEC Broadband Platform: System Architecture and Software Implementation”, Seismological Research Letters, Vol. 86, No. 1, doi: 10.1785/0220140125.

Montero, W., Pardo, M., Ponce, L., Rojas, W., and Fernández, M. (1994). “Evento principal y réplicas importantes del terremoto de Limón”. Revista Geológica de América Central, Volumen Especial del Terremoto de Limón. (pp. 93-102).

Morales, L. (1994). “Daños causados por el terremoto de Limón: Pérdidas y medidas de mitigación”. Revista Geológica de América Central, Volumen Especial del Terremoto de Limón. (pp. 201-210).

Moya, A. (2018). “Cálculo de la intensidad JMA para registros de movimiento fuerte del Laboratorio de Ingeniería Sísmica en Costa Rica”. Revista Internacional de Desastres Naturales, Accidentes e Infraestructura Civil. Vol. 18 (1-2), 29

Muñoz-Barrantes, J., Vargas, L., Cubillo, P., and Vega, P. (2017). “Protocolo de inspección de puentes después de sismo”. https://www.lanamme.ucr.ac.cr/repositorio/handle/50625112500/936 last accessed June 01, 2021.

O’Rourke, M., and Ballantyne, D. (1992). “Observations on water system and pipeline performance in the *Limón* area of Costa Rica due to the April 22, 1991 earthquake”. Technical Report NCEER-92-0017. National Center for Earthquake Engineering Research.

Plafker, G., and Ward, S. (1992). “Backarc thrust faulting and tectonic uplift along the Caribbean sea coast during the April 22, 1991 Costa Rica earthquake”. Tectonics, 11, 709-718.

Protti, M., González, V., Newman, A., Dixon, T., Schwartz, S., Marshall, J., Feng, L., Walter, J., Malservis, R., and Owen, S. (2014). "Nicoya earthquake rupture anticipated by geodetic measurement of the locked plate interface", Nature Geoscience, 7(2), 117–121.

Quesada-Román, A. (2017). "Impactos geomorfológicos del terremoto de Limón (1991; Ms 7.5) y consideraciones para la prevención de riesgos asociados en Costa Rica". Revista Geográfica de América Central, 56, pp. 93-111.

Santana, G. (1994). "The April 22, 1991 Limón (Costa Rica) earthquake". Earthquake Engineering, Tenth World Conference, Balkema Rotterdam, ISBN 9054100605.

Sauter, F. (1994). "Evaluación de daños en puentes y otras estructuras civiles causados por el terremoto de Limón". Revista Geológica de América Central, Volumen Especial del Terremoto de Limón. (pp. 171-186).

Schmidt, V. (2014). "Clasificación de suelos de 15 estaciones acelerográficas, mediante el uso de métodos basados en vibraciones ambientales y del parámetro Vs30". Revista Geológica de América Central. No. 51, pp.33-67. ISSN 0256-7024.

Schmidt, V., Hidalgo, D., Acuña, A., Moya, A., Cordero, E., Segura, C., and López, E., (2014), "Aceleraciones del terremoto de Sámara del 05 de setiembre del 2012", Nota Técnica, Revista En Torno a la Prevención, Comisión Nacional de Emergencias, No. 12, pp. 38-47.

Shabestari, K., and Yamazaki, F. (2001). "A Proposal of Instrumental Seismic Intensity Scale Compatible with MMI Evaluated from Three-Component Acceleration." Earthquake Spectra, Vol. 17, No. 4, pp 711–723

Suárez, G., Pardo, M., Domínguez, J., Ponce, L., Montero, W., Boschini, I., and Rojas, W. (1995). "The Limón, Costa Rica earthquake of April 22, 1991: Back arc thrusting and collisional tectonics in a subduction environment". Tectonics, 14(2), 518–530.

Wessel, P., Smith, W. H. F., Scharroo, Luis, J. F., and Wobbe, F. (2013). "Generic Mapping Tools: Improved version released", EOS Trans. AGU, 94, pp. 409-410.